# Low voltage power grid congestion reduction using a community battery
## Design principles, control and experimental validation

van Westering, Werner; Hellendoorn, Hans

**DOI**
10.1016/j.ijepes.2019.06.007

**Publication date**
2020

**Document Version**
Final published version

**Published in**
International Journal of Electrical Power and Energy Systems

Electrical Power and Energy Systems 114 (2020) 105349

Contents lists available at ScienceDirect

Electrical Power and Energy Systems

journal homepage: www.elsevier.com/locate/ijepes

# Low voltage power grid congestion reduction using a community battery: Design principles, control and experimental validation

Werner van Westering[a,b], Hans Hellendoorn[a]

[a] Delft Center of Systems & Control, Delft University of Technology, Delft Mekelweg 2, 2628CD, The Netherlands
[b] Alliander N.V., Duiven, Dijkgraaf 4, Postbox 50, 6921 RL, The Netherlands

ARTICLE INFO

*Keywords:*
Distribution grid
Energy transition
Electricity storage
Battery
Community battery

ABSTRACT

By installing a battery storage system in the power grid, Distribution Network Operators (DNOs) can solve congestion problems caused by decentralized renewable generation. This paper provides the necessary theory to use such a community battery for grid congestion reduction, backed up by experimental results. A simple network model was constructed by linearizing the load flow equations using a constant impedance load model. Using this model, an accurate estimate of voltage and overload problems is fed into a receding horizon charge path optimizer. The charge path optimization problem is posed as a linear problem and subsequently solved by an LP solver. The algorithms have been applied and validated on a real-world community battery installation. It was found that the voltages and currents can be controlled to a great degree, increasing the grid capacity significantly. The proposed control framework can be used to safeguard network constraints and is compatible with other battery control goals, such as energy trading or energy independence. Network design formulas are described with which a DNO can quickly estimate the potential (de) stabilization of a community battery on the steady-state voltages and currents in the grid.

## 1. Introduction

The energy landscape is expected to change significantly in the Netherlands over the next decades, as the share of renewable energy is increasing. This poses a significant challenge for Distribution Network Operators (DNOs), which are responsible for maintaining a reliable and affordable electricity distribution grid. Especially the rise of residential solar power is challenging, as these installations can cause local voltage problems which can be cost intensive to solve.

A potential solution to this problem is congestion control using energy storage. By locally storing the energy generated by the solar power installations, the voltage and current in the low voltage network can be kept within the desired bounds. The most common version of this solution is a home battery system. However, it is more efficient to use a community battery since the home batteries are often not fully utilized [1,2]. A community battery also requires less space and can be serviced more efficiently.

However, DNOs do generally not have the knowledge to design and employ a community battery, which results in both newly planned and currently installed storage capacity not being used for congestion control. This paper provides the necessary theory to solve this problem, backed up by experimental results. With the principles developed in this paper, a DNO can quickly estimate the potential (de) stabilization of a community battery on the steady-state voltages and currents in the grid. The control framework provided can be used to safeguard network constraints and is compatible with other battery control goals, such as energy trading or energy independence.

For experimentation purposes Liander, the largest DNO of the Netherlands serving over three million customers, placed a community battery in Rijsenhout, a suburban village close to Amsterdam, the Netherlands. A schematic overview of the network of Liander DNO is displayed in Fig. 1. The battery is connected to the low voltage network and has a peak power of 55 kW and a capacity of 126 kW h. The main goal of placing the battery was the broad goal of obtaining practical knowledge how a community battery can benefit the DNO.

This paper reports on various aspects of DNO community battery utilization. It contains control strategies for using a community battery for LV network congestion management. It is the first study to combine a battery control system with a real time grid model. It also analyses the battery's (de) stabilization potential and provides design guidelines for new community batteries.

## 2. Related work and contributions

Using batteries in addition to a regular connection to the power grid is a relatively new phenomenon in Western Europe, because grid

*E-mail addresses:* w.h.p.vanwestering@tudelft.nl, werner.van.westering@alliander.com (W. van Westering).

https://doi.org/10.1016/j.ijepes.2019.06.007
Received 15 February 2019; Received in revised form 7 May 2019; Accepted 3 June 2019
Available online 27 June 2019

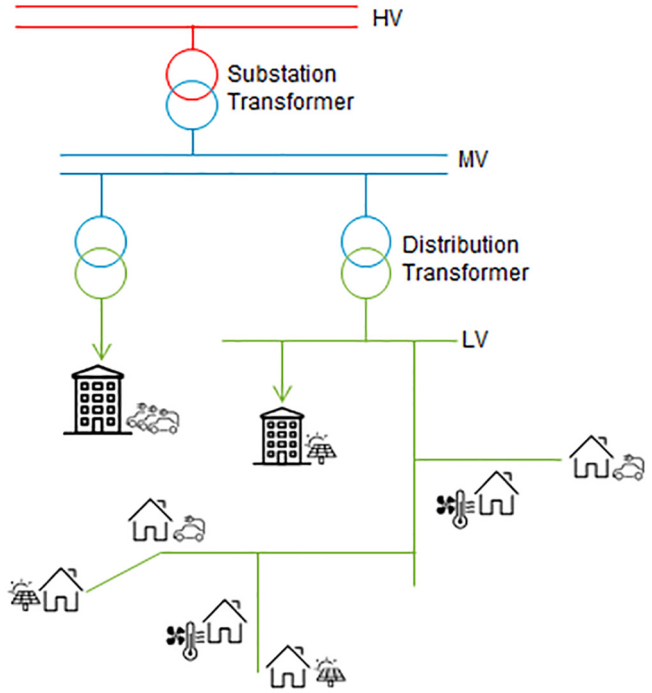


**Fig. 1.** A schematic overview of the voltage levels of the network of Liander DNO. Liander operates the Low Voltage (LV) and Medium Voltage (MV) networks. These networks operate on 400 V/230 V and 10 kV respectively. The High Voltage (HV) network is not operated by Liander DNO. The LV network is the main subject of this study.

connections are very stable and relatively cheap. With the rise of decentralized renewable power generation in the power grid however, grid investment costs are expected to rise sharply [3–5]. This is a strong motivation for the DNOs to explore innovative solutions, such as battery storage.

Many studies try to find interesting new business cases for batteries. Using electric vehicles for electricity storage purposes is not yet feasible [6]. Most work regarding Battery Energy Storage Systems (BESS) focuses on residential applications [7–11]. However, Parra [1,2] calculates that a community battery is 56% cheaper than separate residential batteries for a 100-home community.

The field of battery load path optimization has been studied in the literature quite extensively. For example, the battery scheduling problem for microgrid operation is investigated by [12–14]. Some of the studies also assume a connection to a larger grid [12] or mainly focus on the optimal size of a battery [15,16].

Various receding horizon controllers for battery charge path optimization have been developed [17,18]. Recently, battery controllers using Model Predictive Control (MPC) have been proposed [7,12]. These controllers can be deployed both centralized or decentralized. However, these controllers generally do not guarantee a stable grid operation as the currents and voltages in the grid are not taken into account. This is also due to the fact that the non-linear load flow equations cannot be directly applied in the quadratic MPC framework. Furthermore, these MPC controllers have yet to be tested in a real world test bed. This paper contributes to the literature by proposing and validating a network model which is directly integrable into the MPC framework.

This is the first study that enhances the load path optimization problem by adding a real time network model, making it more interesting for a real world application. Most of the current algorithms work with predefined congestion points, i.e. network nodes which are expected to be most vulnerable to capacity or voltage problems. However, in practice the points are often hard to clearly define for large networks in which the loads are constantly changing. Therefore adding a network model which is able to monitor all network nodes and lines simultaneously is a valuable addition to the current literature.

Furthermore, not much literature is available on applying and validating proposed algorithms on real world batteries. The community battery subject of this study is only the second ever in the Netherlands. The first one was placed by the Dutch DNO Enexis and has been used for validating a charge path optimization algorithm, reducing network losses and reducing transformer peak load [19–21]. However, since the battery was located next to the DT transformer, the ability to influence the LV network was very limited in contrary to the community battery subject of this paper.

Most DNOs have design rules regarding LV network design, but do not have policies available regarding electricity storage as it is a relatively new phenomenon in MV/LV grids. This paper contributes to literature by both providing a battery controller and describing community battery network design guidelines, specifically aimed at DNOs.

## 3. Methodology

Fig. 2 contains a schematic of the battery controller. The rest of this paper is structured as follows: To calculate the characteristics of the LV network, a linear low voltage network model is constructed in Section 3.1 and 3.2. After the linearization is motivated in Section 3.3, the battery control problem is formulated in Section 3.4. The models are applied to the community battery of Rijsenhout and the results and accuracy of these models is investigated in Section 4. The results of the experiments are used to formulate battery design principles in Section 5 and are again applied in Section 6.

### 3.1. Low voltage network model

For monitoring overheating due to large currents and meeting voltage regulations, it is generally sufficient to model on a time scale of several minutes. The standard way to model such an electricity grid on this time scale is the load flow model [22,23]. A load flow problem is generally nonlinear, due to its power constraints. This makes solving the necessary equations computationally expensive.

The standard approach for modeling DNO power grids is formulating a load flow problem and solving it using a Newton-Raphson methodology [22,23]. Usually the load is modeled as a combination of a constant power, constant impedance and constant current [23]. This paper however proposes a simple linear load flow approach by only using a constant impedance load model and investigates its feasibility in a real world situation.

To create the constant impedance model as in Fig. 3, it is necessary to convert the power use of a customer into an equivalent resistance. This can be done by the following formula:

$$Z_{\text{eq}} = U_{n,\text{ref}}^2 / P_{\text{user}} \quad \forall\, n \in \mathcal{N} \tag{1}$$

Here $Z_{\text{eq}}$ is the equivalent resistance of the customer, $P_{\text{user}}$ the real

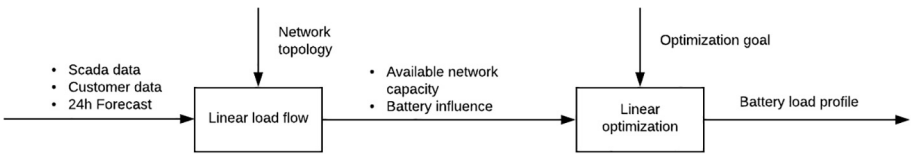


**Fig. 2.** Schematic view of the Community Battery controller.

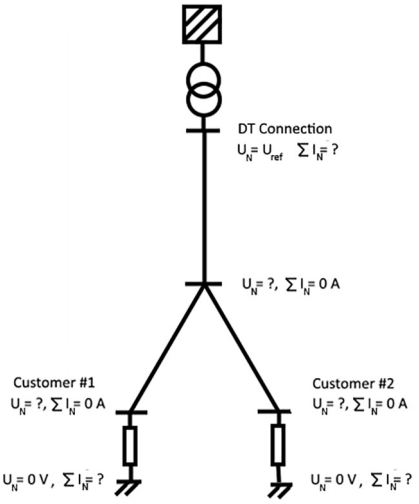


**Fig. 3.** A small example low voltage network. The network has two customers modeled as resistors and a single connection to the medium voltage grid.

power consumption of the customer, $n$ is a bus which represents a customer connection and $U_{n,\text{ref}}$ is the voltage at the customer location. Since the voltage at the customer is usually not known, the reference voltage is be assumed to be the nominal voltage.

From Fig. 3 it can be observed that all nodes on the end of the network are now defined as swing buses, i.e., fixed voltage points. As the power constraints are replaced by resistances, the network now only consists of voltage sources, ground connections and resistors, resulting in a fully linear model.

The network is modeled as a graph. A standard way to define such a graph is by defining graph $G$ as $G = (\mathscr{N}, \mathscr{E})$, where $\mathscr{N}$ are the nodes and $\mathscr{E}$ are the network edges. In case of an electricity network $\mathscr{N}$ represent the network buses and $\mathscr{E}$ are the network cables. The goal of the model is to determine the cable currents $I_{\mathscr{E}}$ and the nodal voltages $U_{\mathscr{N}}$.

The network voltages and currents can be obtained by using Ohm's law:

$$I_{\mathscr{N}} = \overline{Y} U_{\mathscr{N}} \tag{2}$$

Here $I_{\mathscr{N}}$ is the current entering a network bus and $\overline{Y}$ is the so-called admittance matrix. The admittance matrix can be directly obtained from the network lay-out using the following formula [24]:

$$\overline{Y} = A Z_{\mathscr{E}}^{-1} A' \tag{3}$$

Here $A$ is a directional connection matrix. Every row corresponds to a network bus. Every column of $A$ corresponds to a network cable. Each cable should have exactly one starting point denoted by a '1' and one end point denoted by '− 1'. It does not matter which bus of $A$ contains the minus sign, as the resulting admittance matrix $\overline{Y}$ will stay the same. $Z_{\mathscr{E}}$ is a square matrix and has the corresponding impedance of each cable and the equivalent resistance of the customers ($Z_{\text{eq}}$) on its diagonal. Since the matrix is diagonal, its inverse can be easily calculated by taking the inverse of every diagonal element.

However, (2) cannot be solved directly, because not all elements are known in neither vector $I_{\mathscr{E}}$ and $U_{\mathscr{N}}$. To overcome this problem, it is practical to segment the problem in two equations which can be solved separately. This can be done by sorting the rows of the matrices $I_{\mathscr{N}}$, $\overline{Y}$ and $U_{\mathscr{N}}$ in such a way that all swing buses are $\in U_1$. The segments are then defined as:

$$I_{\mathscr{N}} = \begin{bmatrix} I_1 \\ I_2 \end{bmatrix}, \overline{Y} = \begin{bmatrix} K & L \\ L' & M \end{bmatrix}, U_{\mathscr{N}} = \begin{bmatrix} U_1 \\ U_2 \end{bmatrix} \tag{4}$$

Since the network is modeled as a set of voltage sources and resistances, Kirchoff's law dictates that $\Sigma I = 0$ on every bus in $U_2$. Therefore $I_2$ is equal to $\bar{0}$. All the voltages on the end nodes, represented by $U_1$ are known. The voltages in $U_1$ are zero, except for the transformer voltage. The load flow equations now become:

$$\begin{bmatrix} I_1 \\ \bar{0} \end{bmatrix} = \begin{bmatrix} K & L \\ L' & M \end{bmatrix} \begin{bmatrix} U_1 \\ U_2 \end{bmatrix} \tag{5}$$

A natural way to solve for $U_2$ is:

$$U_2 = -M^{-1}(L' U_1) \tag{6}$$

However, matrix $M$ is usually too large and too costly to invert. Fortunately, it is not necessary to compute $M^{-1}$. Instead, it is more practical to solve:

$$L' U_1 = -M U_2 \tag{7}$$

Since this equation is in the form $Ax = B$ it can be solved in many practical ways e.g. a sparse QR decomposition. Finally after computing the voltages, the cable currents can be directly calculated by:

$$I_{\mathscr{E}} = Z_{\mathscr{E}} A' U_{\mathscr{N}} \tag{8}$$

### 3.2. Simulating reactive power in terms of only real numbers

Not all simulation environments can solve complex numbers. For example, the programming language *R* and the Matlab PLC compiler have out-of-the-box support for solving matrices which are both sparse and complex. In these cases, it is beneficial to simulate the imaginary parts of the load flow simulation in terms of only real numbers.

To add reactive power to the load flow simulation, the cable reactances are added to $Z_{\mathscr{E}}$, such that elements of $Z_{\mathscr{E}}$, $Y$, $U$ and $I \in \mathbb{C}$. To include these efficiently in (2), it can be expanded [25,26] to:

$$\begin{bmatrix} I_{\mathbb{R}} \\ I_{\mathbb{C}} \end{bmatrix} = \begin{bmatrix} Y_{\mathbb{R}} & -Y_{\mathbb{C}} \\ Y_{\mathbb{C}} & Y_{\mathbb{R}} \end{bmatrix} \begin{bmatrix} U_{\mathbb{R}} \\ U_{\mathbb{C}} \end{bmatrix} \tag{9}$$

where the subscripts $\mathbb{R}$, $\mathbb{C}$ are used to indicate respectively the real and imaginary part of the matrix. Thus, $Y_{\mathbb{R}} = \text{Re}(Y) = A\text{Re}(Z^{-1})A'$, and correspondingly $Y_{\mathbb{C}} = \text{Im}(Y)$.

Using the same method as before this can be simplified to:

$$\begin{bmatrix} M_{\mathbb{R}} & -M_{\mathbb{C}} \\ M_{\mathbb{C}} & M_{\mathbb{R}} \end{bmatrix} \begin{bmatrix} U_{\mathbb{R},2} \\ U_{\mathbb{C},2} \end{bmatrix} = -\begin{bmatrix} L_{\mathbb{R}} & -L_{\mathbb{C}} \\ L_{\mathbb{C}} & L_{\mathbb{R}} \end{bmatrix} \begin{bmatrix} U_{\mathbb{R},1} \\ U_{\mathbb{C},1} \end{bmatrix} \tag{10}$$

which is the complex variant of the equation $MU_2 = LU_1$. By solving this equation, the voltages can be determined. Eq. (9) can be used to find the currents through the cable-segments. Then $U_{\mathscr{N}}$ and $I_{\mathscr{N}}$ can be found by:

$$U_{\mathscr{N}} = \sqrt{U_{\mathbb{R}}^2 + U_{\mathbb{C}}^2} I_{\mathscr{N}} = \sqrt{I_{\mathbb{R}}^2 + I_{\mathbb{C}}^2} \tag{11}$$

### 3.3. Motivation for linear modeling

The LV networks are generally very well conditions for linear simulations. Compared to the MV network, they consist of relatively short cables with a low X/R ratio. As can be derived from (1), the difference between the non linear constant power model and the constant impedance model is caused by the voltage drop i.e. the difference of the estimated voltage $U_{n,\text{ref}}$ and the actual voltage $U_n$. According to Dutch law and Alliander DNO policies, the voltage drop in the LV network is not allowed to be more than 4.5%, resulting in a worst case difference in absolute voltage of less than 1 V in a network which operates on 230 V and has a 4.5% voltage drop. However, the linearization quickly loses its accuracy as the voltage drop gets higher and is only to be applied on networks with a relative small voltage drop.

On a side note, it can be argued that modeling the customers as a constant impedance load model is not necessarily less accurate as a constant power load model. In reality, customers will have a mix of devices which require a constant power load, such as home computers and TVs, and devices which are in reality a constant impedance load,

such as boilers and heaters.

The main reasons for linearizing the load flow model are the improvement in speed and stability regarding a non linear model. Because since the load flow equations can be solved without iterative methods, it can be solved for large networks in a very short time span [25]. This makes it viable for control purposes, as it can be used to evaluate many different control strategies. Computational power is often an expensive resource in a control environment. For example, the local controller of the community battery has a clock speed of 500 MHz and 64 MB RAM, which is very slow compared to a modern PC.

Regarding model stability, a linear network model it is not prone to finding unfeasible solutions or numerical difficulties, which can occur in normal load flows [23]. Given that stability of a controller is essential, this property makes the linear method more suitable for control.

While in most cases the LV network is radial, this is not necessarily always the case. There are low voltage networks in Liander DNO area which are operated in a non-radial manner and sometimes span over a thousand kilometer of cable and supply tens of thousands of households. It happens that the load flow equations as formulated in this paper are directly applicable to these large LV grids, while maintaining good performance [5].

A final advantage of a linear network model is its linear additive property, which means that each network load configuration can be simulated independently. In practice this means that all loads can be simulated separately and the resulting voltage drop and cable currents can be obtained by simply taking the sum of all solutions. This property will be exploited in next section to efficiently determine the maximum power the battery supply to or draw from the network.

A small downside of the constant impedance model is that it is prone to computational errors when a customer's power consumption is very close to zero. As can be seen in (1), if the power consumption is zero, the equivalent resistance is infinite. In practice, this problem can be easily solved by ensuring that the power consumption of each customer is always a few watts, which has a negligible influence on the outcome of the simulation.

### 3.4. Formulating the battery control problem

Given the model of the LV network and the framework of Fig. 2, the next step is to formulate a battery controller which safeguards the voltage and current constraints of the network while being compatible with other control goals, such as day-trading. Furthermore the algorithm has to be stable and operable in real-time.

The controlled variable is the battery power at each time step $P_t$. The final goal of the controller is to keep the battery at a certain given charge level $E_{t,\mathrm{ref}}$. This desired charge level is given by another entity, like a day-trader who is using the battery for energy trading. The optimization function is now posed as a discrete receding horizon problem. The objective function becomes:

$$\underset{P_t}{\text{minimize}} \quad \sum_{t=1}^{T} \left| E_t - E_{t,\mathrm{ref}} \right| \tag{12}$$

The power the battery can inject in or draw from the network is limited by its rated power $P_{\mathrm{bat}}$, but also by the network voltages at each customer bus ($U_c \ \forall\, c \in \mathscr{N}$) and network currents $I_E$. These constraints have to be satisfied at every time step $t$ in prediction horizon $T$. $E_t$ is the energy in the battery at time step $t$. The first step is to apply the load flow model to this optimization problem.

Because the constructed load flow model is linear, network states can be evaluated independently using the principle of superposition. This is useful, as the impact of the network load on the voltages and currents can be calculated separately from the impact of the battery power. The maximum and minimum battery power can therefore be obtained by dividing the available voltage drop by the voltage drop caused by the battery at 1 W. Since the network is only as strong as its weakest connection; the weakest cable or bus determines the boundaries of the battery. These boundaries can be calculated with the following formulas:

$$\begin{aligned} P_{U,\max,t} &= \min \frac{U_{\max} - U_{n,t}}{\Delta U_{P_{\mathrm{W},n}}} \qquad \forall\, n \in \mathscr{N},\ tP_{U,\min,t} \\ &= \max \frac{U_{\min} - U_{n,t}}{\Delta U_{P_{\mathrm{W},n}}} \qquad \forall\, n \in \mathscr{N},\ t \end{aligned} \tag{13}$$

Here $P_{U,\max,t}$ and $P_{U,\min,t}$ are the maximum and minimum power the battery is allowed to inject into the network at time $t$ without violating any voltage limits, $U_{\max}$ and $U_{\min}$ are the maximum and minimum allowed voltage at each customer by law. $U_{n,t}$ is the voltage at each customer which can be calculated by solving (2).

$\Delta U_{P_{\mathrm{W},n}}$ is the voltage drop by applying 1 W of battery power to the grid in V/W. This variable is time-invariant and only depends on the network properties. The number can be obtained by solving by setting the battery power to 1 W, setting the customer power to a low but nonzero value and solving (2). The customer load cannot be set to zero as most QR solvers cannot cope with infinite resistances. $\Delta U_{P_{\mathrm{W},n}}$ is network-dependent and does not vary over time.

For monitoring currents similar formulas exists:

$$\begin{aligned} P_{I,\max,t} &= \min \frac{I_{\max,e} - I_{P_t,e,t}}{I_{\Delta P_{\mathrm{W},n}}} \qquad \forall\, e \in \mathscr{E} P_{I,\min,t} \\ &= \max \frac{I_{\min,e} - I_{P_t,e,t}}{I_{\Delta P_{\mathrm{W},e}}} \qquad \forall\, e \in \mathscr{E} \end{aligned} \tag{14}$$

Here $P_{I,\max,t}$ and $P_{I,\min,t}$ are the maximum and minimum power the battery is allowed to inject into the network at time $t$ without violating any current limits. $I_{\max,e}$ and $I_{\min,e}$ are the maximum and minimum allowed currents at cable $e$. $I_{P_t,e,t}$ is the current at each cable which can be calculated by solving (2) and applying (8). $I_{\Delta P_{\mathrm{W},e}}$ is the current change per 1 W of battery power applied to the grid in A/W. Just like the $\Delta U_{P_{\mathrm{W},c}}$ this variable is time-invariant and only depends on the network properties.

The battery has also a maximum rated power. The full network-related constraints are now defined as:

$$\begin{aligned} P_{\max,t} &= \min(P_{\max,t,U},\ P_{I,\max,t},\ P_{\mathrm{bat},\max,t}) P_{\min,t} \\ &= \max(P_{\min,t,U},\ P_{\min,t,I},\ P_{\mathrm{bat},\min,t}) \end{aligned} \tag{15}$$

The optimization problem with added constraints becomes:

$$\begin{aligned} \underset{P_t}{\text{minimize}} \quad & \textstyle\sum_{t=1}^{T} |E_t - E_{t,\mathrm{ref}}| \\ \text{subject to} \quad & P_{\min,t} \leqslant P_t \leqslant P_{\max,t} \qquad \forall\, t \in T \\ & 0 \leqslant E_t \leqslant E_{\max,t} \end{aligned} \tag{16}$$

Here $P_t$ is the real power the battery supplies to the electricity network at timestep $t$. $E$ is the energy stored in the battery, which cannot exceed $E_{\max}$. The first constraint corresponds to the network-related power limit. The second constraint ensures that the battery will not discharge when it is empty and not charge when it is full. If all the currents and voltages are within their boundaries, the battery does not need to act. However, if an undesired value is found, the battery will try to mitigate the problem.

However, the formulated problem can not directly be put in a linear solver in its current form. To solve the problem using a linear solver, it is necessary to incorporate the absolute term of the objective function into the constraint function. This is achieved by adding an extra dummy variable $\overline{E}$.

Also, the required voltage and current boundaries may be unattainable, because of the practical limitations of the battery. In such a situation, the linear solver will not find a feasible solution and the battery will be inactive. A more desirable behaviour is in a practical case to meet the required voltage and current constraints as much as possible.

To this end, a barrier function has been implemented. The barrier function gives a large penalty for violating the voltage and current boundaries, barely influencing the regular optimization. In case of unattainable requirements, the solver will still find a solution which violates the constraints as little as possible. The variable corresponding to the barrier function is $P_{\text{over}}$. This function is given a large weight $c$, where $c \gg \overline{E}$.

The definitive optimization problem now becomes:

$$\begin{aligned} \underset{E_t, \overline{E}, P_{\text{over}}}{\text{minimize}} \quad & \overline{E} + c \cdot P_{\text{over}} \\ \text{subjectto} \quad & \overline{E} + E_t \geqslant E_{\text{ref}} \qquad \forall\, t \in T \\ & \overline{E} - E_t \leqslant E_{\text{ref}} \\ & 0 \leqslant E_t \leqslant E_{\text{max},t} \\ & E_{t+1} - E_t - P_{\text{over},t} \leqslant P_{\text{max},t} \\ & E_{t+1} - E_t + P_{\text{over},t} \geqslant P_{\text{min},t} \\ & E_1 = E_{\text{start}} \end{aligned} \tag{17}$$

This problem can be directly solved by a linear optimization solver. Since the problem is linear, the solution will be optimal if it is found. If the constraints do not conflict with each other, the solution always exists.

Since the battery controller is designed with a horizon of several days, the energy lost by the self-discharging of the battery is neglected. Furthermore, the load cycle efficiency of the battery is also neglected, as it is known to be over 90% in normal operating ranges. To mitigate the inaccuracies caused by these assumptions, $E_{\text{start}}$ has to updated at every optimization step using the measurement of the state of charge of the battery provided by the battery management system.

## 4. Experimental setup part I: The community battery of Rijsenhout

Liander, the largest DNO of the Netherlands serving over three million customers, placed a community battery in Rijsenhout, a suburban village close to Amsterdam, the Netherlands. The battery is connected to the low voltage power grid as can be seen in Fig. 4. The community battery has a usable energy rating of 126 kW h and a 55 kW peak power rating. The battery itself is capable of a higher power output, but safety regulations required the 55 kW limit.

Using the conventional load flow software and modeling assumptions of Liander DNO, an analysis of the network of Rijsenhout showed that the network was expected to have no voltage or capacity problems. However, during the experiments it became clear that the conventional modeling assumptions were incorrect and the network was subject to voltages which were too high according to regulations. Sensor data proved that the voltage problems were caused by fluctuations of the voltage on the medium voltage grid, which directly influenced the voltage of the low voltage power grid and exceeded the modeling assumptions. However, this situation provided an excellent opportunity to prove that the battery could also mitigate the voltage problems. Dutch inverters are required to automatically switch off in the event the voltage is above 250 V to mitigate voltages and this threshold was exceeded on a regular basis.

During the experiment, only active power was considered because very little reactive power could be expected to be present in this LV network. The customers in this network are regular households, which are known to consume little reactive power. Also, the X/R ratio of the cables in the network is very low, making the phase angle nearly constant in the entire network. There is also a practical reason for neglecting reactive power as the installed sensors only logged real power.

To make the experiment broader than just the DNO perspective, an additional control objective was formulated. Most of the customers have their own PV installation, and by aggregating their consumption and defining it as $E_{\text{ref}}$, the customers can 'live on their own solar energy' as much as possible. This is also of interest to the DNO as it mitigates peak loads from other network areas.

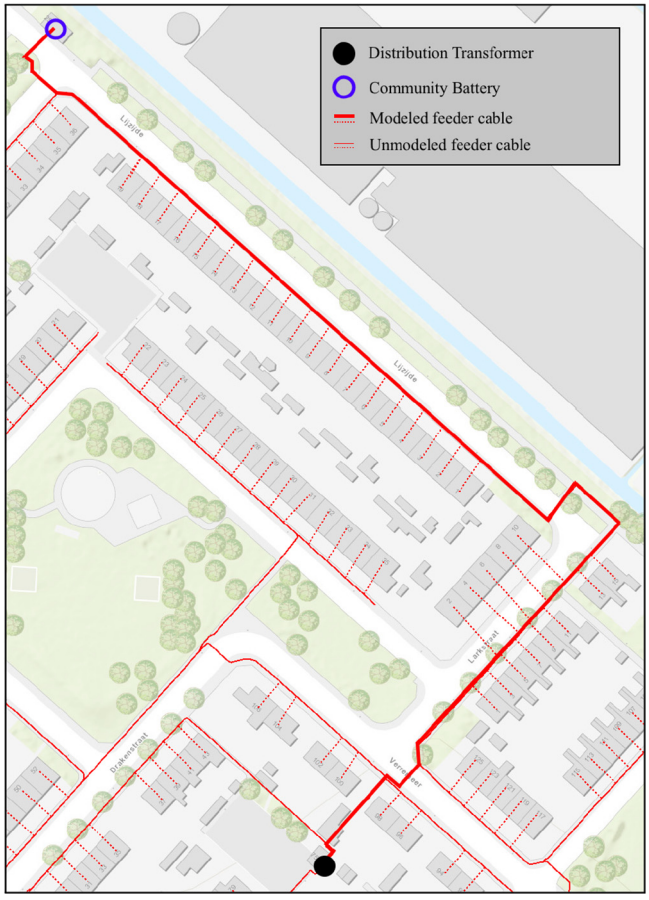


**Fig. 4.** GIS view of Liander's low voltage network of Rijsenhout [27]. The outlined modeled network is the feeder that is considered for the LV model. The unmodeled cables are not physically connected to the modeled network, except for a connection in de DT transformer.

### 4.1. Optimization results

At the distribution transformer and the community battery both power and voltage are measured. The modeled part of the network consists of 34 customers. At 12 households, the power was measured. For privacy reasons, their exact location could not be displayed, but they are almost uniformly distributed along the cable. The data which is displayed in this section is averaged on the time scale of one minute.

Fig. 5 shows the result of the attempt to make the LV network self-sufficient. The community battery did most work in August, nearly doubling the self-consumption of the generated solar energy within the

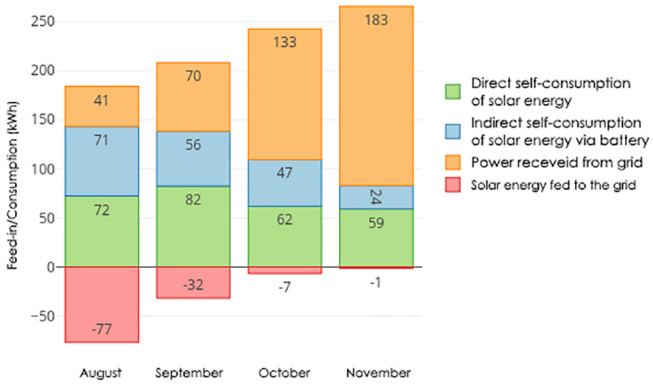


**Fig. 5.** Source of the electricity of a single average customer in the community battery LV grid from August 2017 to November 2017.

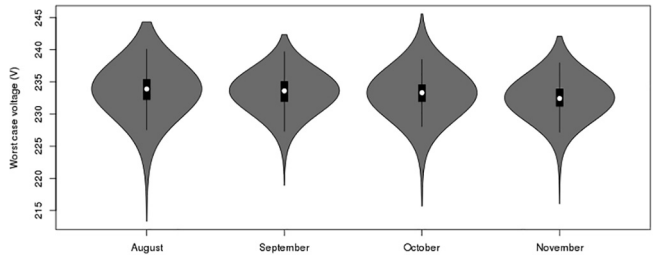


**Fig. 6.** Measured voltages at the community battery in the network from August 2017 to November 2017. The LV voltage never exceeds the bounds of 245 V and 215 V as required.

LV grid. Still 77 kW h per household could not be stored in the battery because of capacity limits in this months. August and September are the two last months of the summer in the Netherlands. In October and November, there was much more power consumption on average and less solar power generation. It can be observed from Fig. 5 that in October and November almost no power was delivered to the grid for this reason. Battery losses (and other transportation losses in general) are not part of Fig. 5, because they have to be compensated by the DNO.

Fig. 6 shows the maximum measured voltage from all available sensors. The battery controller keeps all voltage within the set bounds of 245 V and 215 V. In September and November, the community battery did not need to act to keep the voltages within the required bounds. During the months the community battery and its controller were active, the maximum network voltage was lowered from previously observed voltage peaks of 250 V to voltage peaks of 245 V, mitigating the voltage problems.

For solving (17), the optimizer depends on a prediction of the power consumption and solar power generation. This prediction is obtained by training a regression model using historical data and was provided by an external party. The model has a Mean Absolute Percentage Error (MAPE) of 5% for predicting household load and 10% for PV power 24 h ahead. During the experiment it was discovered that the accuracy of the energy consumption predictions is relatively unimportant. The controller anticipates on high demand or load by reserving capacity of the battery. Using this available energy and the available real-time measurements, the controller then reacts to the voltage/current problems once they actually arise. It turns out that the most important prediction feature is the required amount of energy to mitigate voltage/current problems, not the exact peak loads.

### 4.2. Checking for linearity

This sections investigates how well the linear constant impedance load flow model applies to low voltage networks. The LV model constructed in the previous sections relies on a main assumption: The load model is assumed to behave as a constant impedance.

To determine if the constant-impedance model is indeed accurate on the voltage range of the LV network, a short experiment was performed. As can be observed in Fig. 7, the battery was given a significant 'saw tooth' shaped load profile as a reference. The charging experiment was performed in a few hours around noon, which is the time with the least power consumption during the day because of the presence of solar panels. The customer power consumption is significantly less than the battery power.

As can be seen in Fig. 7, the battery ramped up and down from 50 kW, its maximum rated power. It can also be concluded that the battery can control the voltage at the end of the LV network either 12 V up or down, covers the entire range of the allowed 4.5% voltage drop on LV networks. To determine the exact relation between battery power and voltage drop, the plot in Fig. 8 was constructed. From this figure, it can be concluded that the relation between battery power and voltage drop can indeed be approached by a linear function within the

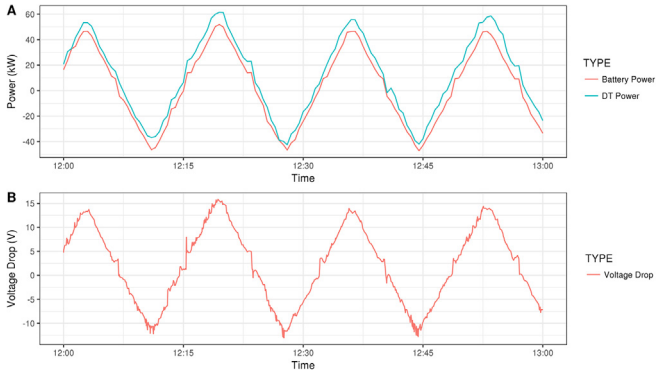


**Fig. 7.** To determine the characteristics of the voltage drop the battery was given a 'saw tooth' shaped charging profile. It can be observed that there is an approximate linear relation between the battery power and the voltage drop between the transformer and the battery.

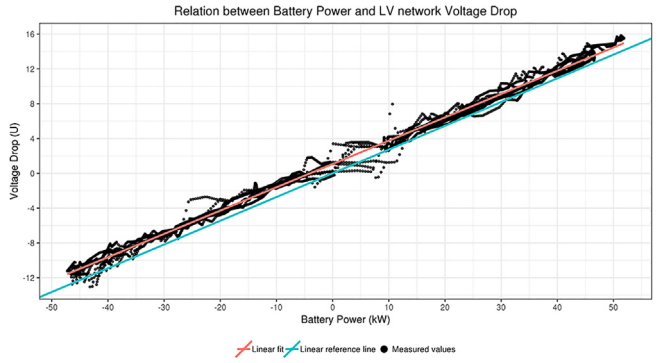


**Fig. 8.** The relation between the Battery Power and the measured voltage drop from the DT to the Battery. The time span of this figure is the same as in Fig. 7. It can be observed that the relation between battery power and voltage drop can be approximated by a linear function.

operating range of the battery.

The deviations around zero battery power, which can be observed in Fig. 7, are caused by the imperfect inverter. The battery inverter cannot behave linearly at very low battery power levels. It can also be observed in Fig. 8 that the linear fit has a slight additive bias. This is caused by the small residual load which also can be observed in Fig. 7.

## 5. Community battery design specifications

The following section contains design principles to quickly determine the key properties of a community battery for network congestion reduction purposes, in new or existing grids. Using the observation of the previous sections, generalized rules have been established. These rules have been designed to be used by network planners and have been kept as simple as possible. It has been assumed that a standard load flow simulation is unavailable to maximize the simplicity of the network analysis. A drawing of the low voltage network is sufficient to apply the proposed rules, once the problem and its size are known.

There are two main motivations considered to place a community battery for network congestion reduction: to control the community voltage and to control the community currents. While it is theoretically possible to also control the network power factor to some extend, this is currently not a priority for distribution network operators, because of its rare occurrence.

A simple but realistic situation is assumed. The network has a relatively simple radial structure and its cable locations and properties are known. It is also assumed that the location and size of the voltage problems are roughly known. These either have been determined using

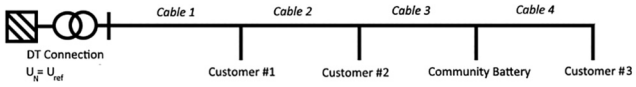


**Fig. 9.** A battery placement example. If a battery is placed at between customer 2 and 3, it can control the currents and voltage drops in cable 1, 2 and 3.

smart meter data or direct (temporary) measurements.

As will be motivated in the following paragraphs, the most important properties of a community battery are:

- The location of the connection of the battery to the low voltage power grid.
- The battery power rating.
- The battery capacity.

The first step in designing a community battery is determining its location. The size of a large battery and its control installation is significant, which strongly limits the number of available placement locations. For example, in the case of the community battery of Rijsenhout the battery size is half a standard shipping container and only a single placement location was available.

Given is the network model of Fig. 9 and the linear relation between battery power and voltage drop as seen in Fig. 8. If one assumes that the customer load is not significantly influenced by the voltage drop, simple approximate formulas can be constructed for battery placement.

In the previous section it was shown that there is a linear relation between battery power and voltage level, which motivates the next formula. Once the location is determined, one can determine the minimal required power rating of the battery with the following formula:

$$P_{\min,U} = \alpha \frac{\Delta U}{l} \tag{18}$$

Here $P_{\min,U}$ is the minimal battery power required to solve the voltage problem (W), $\Delta U$ is the size of the largest voltage problem (V) i.e. the node which has the largest gap between the allowed voltage ($U_{\max}$) and its maximum measured voltage. $l$ is the length of the part of the cable which is shared by both the customer with the largest voltage problem and the community battery (m). For example, if in Fig. 9$\Delta U$ is located at customer 2, then $l = l_{\text{Cable1}} + l_{\text{Cable2}}$. $\alpha$ is a cable dependent factor ($\frac{\text{m}}{\text{W·V}}$) which represents the average cable resistance per meter. It can be obtained by the formula: $\alpha = U_{\text{ref}}/\rho$. Here $U_{\text{ref}}$ is the reference voltage (V) and $\rho$ is the cable specific resistance ($\Omega$/m). $\alpha$ is used instead of adding $U_{\text{ref}}$ and $\rho$ to (18), making it easier to construct a look-up table for engineers. As a general guideline, a community battery should be connected with the longest possible path to the MV/LV transformer. Or to put in another way, the community battery should share as much meters of cable with the customers as possible.

To determine the minimum power required to mitigate current problems and given the network model's assumptions, the following formula is proposed, assuming that the power will mainly flow between the DT transformer and the battery:

$$P_{\min,I} = U_{\text{ref}} \cdot \Delta I \tag{19}$$

Here $\Delta I$ is the size of the largest current problem, i.e. the difference between the actual current and the maximum cable capacity. It is essential that this current problem is situated on the cable between the battery and the distribution transformer or else the battery power will have negligible effect on this particular current. For example, if in Fig. 9$\Delta I$ is located at customer 3, then the community battery cannot solve this problem.

The minimal required battery power now becomes:

$$P_{\min} = \max P_{\min,U}, P_{\min,I} \tag{20}$$

It can be concluded from (18) and its underlying equations, that the location of the battery is its most critical aspect. (20) shows that the location has great impact on the required amount of battery power regarding voltage problems. Because of the linear property of (18), a battery placed twice as far away from the MV/LV connection generally needs only half the power rating. Current problems cannot be influenced at all if the battery is not in the correct position, as (19) requires the overcurrent to be between the transformer and the battery itself.

Once the minimal required battery power has been determined, one can determine the required battery storage capacity. The storage capacity should meet two criteria; it should be sufficiently large to provide the requested power and solve the voltage or current problem. These criteria are displayed in (21) and (22) respectively.

$$E_{\min} = |P_{\min}| \cdot C \tag{21}$$

In this formula $E_{\min}$ is the minimal required storage capacity (kW h). $C$ is the so-called C-value [28], a factor which expresses the relation between battery power and capacity (kW h/kW). This factor is mostly technology dependent and can be as high as 3 for lithium-ion batteries [29]. The second criterion is:

$$E_{\min} = \frac{1}{t_s} \sum_{i=1}^{n} P_{\min,i} \tag{22}$$

Here $t_s$ is the sampling period, $n$ the number of samples and $P_{\min,i}$ the required battery power at time step $i$. The formula should be applied for the duration of the voltage/current largest problem. Since community batteries are generally not meant for seasonal storage, it is sufficient to sample several days.

Using the newly determined properties of the community battery, a cost-benefit analysis can be easily obtained because location, power rating and capacity are also the most important factors for battery costs. The exact break down of the operational and capital costs of the battery and its comparison to conventional network strengthening methods are beyond the scope of this paper.

## 6. Experimental setup part II: Dimensioning the community battery of Rijsenhout

In this section, the previously proposed formulas are applied on the community battery of Rijsenhout as an example. While studying the network of Rijsenhout, it was discovered that the largest voltage problem is 5 V. The location of this problem is at the customer closest to the community battery. Applying (18) results in a required battery power of 15 kW. This is much less than the battery's rated power of 50 kW. No current problems were measured in the network of Rijsenhout, so (19) does not need to be applied.

At its worst, the voltage problem was present for several hours. Determining the required capacity by applying (22) yielded a required capacity of 35 kW h. However, given a C-value of 3 and using (21), the minimal required capacity turns out to be at least 45 kW h. This is also much less than the rated capacity of 125 kW h. It turns out the community battery of Rijsenhout could have been approximately 50% smaller.

It is interesting to note that the optimal location for stabilizing the battery is the inverse of the optimal location for day trading. (18) shows that a battery has a larger influence on the voltage if it is further away from the transformer. While this is a desirable trait if the battery is used for network stabilization, a battery used primarily for day trading should be placed as close to the transformer as possible to minimize the impact on the grid. However, regarding voltage problems the negative impact of day trading can be partly mitigated by using the reactive power control capabilities of a battery inverter. These capabilities were not available in this field test and are therefore beyond the scope of this paper.

Furthermore, (18) can also be used to determine the potential destabilization of the grid. For example: Given the fact that the

community battery of Rijsenhout can control the voltage 12 V and that the maximal measured voltage in the LV network is already 250 V, the community battery can easily cause voltages of over the legal limit of 253 V. To be able to estimate this problem is of great use for DNOs, as it proves that the battery power levels cannot be left unmonitored.

## 7. Conclusion

This paper provides a solid foundation for integrating residential and community-level storage in the existing LV network. A fast linear LV model was developed and applied to the LV feeder of the community-battery in Rijsenhout. The model was proven to be sufficiently accurate for network stabilization purposes.

The battery control theory was formulated as a linear optimization problem. A receding horizon controller was developed to be used in a continuous way. The controller is suited very well to be integrated with other battery control goals, while still securing the voltages and currents within the network. It has been shown that a community battery is able to stabilize and control the loads in a real world low voltage network to a large extend.

A step-by-step method was proposed for quickly modeling the impact of new and existing batteries on the LV grid. Both the stabilizing and destabilizing potential regarding steady-state voltages and currents of the battery can be quickly estimated. By unlocking the potential of battery storage on a DNO level, a fast and secure energy transition is one step closer.

### 7.1. Future research

Being able to control such a large battery to freely test control algorithms provides many opportunities for future research. Next steps will include the application of state estimation algorithms to optimize the estimates of the voltages and currents and also properly account for uncertainties in network measurements and properties.

Furthermore, relatively little is known about the exact nature of low voltage network load. It is the author's ambition to create an accurate load model by applying system identification methods, using the community battery as a means to 'excite' the network to find the voltage and current dependability of the power loads. This could result in a general method for DNOs to identify the load types of their networks.

As additional validation, the theoretical network design formulas proposed in this paper will be tested on more test beds. A test bed of 50 residential batteries is currently in development. Researchers are welcome to contact the corresponding author of this paper to see if their own algorithms can be tested at our facility.

## Acknowledgment

The authors give special thanks to the community battery project team at Liander, without this research would not have been possible. The team provided the actual experimental setup from design to realization, a process which took over a year. The project team consisted of: Jan Willem Eising, Hans Beckers, Rob van Olst, Sander Schoot Uiterkamp, Paul Albers, Dieneke van der Berg, Olaf de Leeuw, Maikel Juriaan Kryzewski, Mike van der Heijden, Mathijs de Groot, Maurice van Duijnhoven, Sidoeri Dekker, Peter Wiebes, Gilbert Smink and Harold Veldkamp. Also thanks to Roel Dobbe and Jacco Heres who provided much valuable feedback. Thanks to Barbera Droste for providing the framework regarding reactive power modeling.

## Appendix A. Supplementary material

Supplementary data associated with this article can be found, in the online version, at https://doi.org/10.1016/j.ijepes.2019.06.007.

## References

[1] Parra D, Norman SA, Walker GS, Gillott M. Optimum community energy storage system for demand load shifting. Appl Energy 2016;174:130–43.
[2] Parra D, Norman SA, Walker GS, Gillott M. Optimum community energy storage for renewable energy and demand load management. Appl Energy 2017;200:358–69. https://doi.org/10.1016/j.apenergy.2017.05.048http://www.sciencedirect.com/science/article/pii/S0306261917305524.
[3] Mallet P, Granstrom PO, Hallberg P, Lorenz G, Mandatova P. Power to the people!: European perspectives on the future of electric distribution. IEEE Power Energy Mag 2014;12(2):51–64. https://doi.org/10.1109/MPE.2013.2294512.
[4] Veldman E, Gibescu M, Slootweg HJ, Kling WL. Scenario-based modelling of future residential electricity demands and assessing their impact on distribution grids. Energy Policy 2013;56:233–47.
[5] van Westering W, Zondervan A, Bakkeren A, Mijnhardt F, van der Els J. Assessing and mitigating the impact of the energy demand in 2030 on the dutch regional power distribution grid. In: 2016 IEEE 13th International Conference on Networking, Sensing, and Control (ICNSC). IEEE; 2016. p. 1–6.
[6] Heymans C, Walker SB, Young SB, Fowler M. Economic analysis of second use electric vehicle batteries for residential energy storage and load-levelling. Energy Policy 2014;71:22–30. https://doi.org/10.1016/j.enpol.2014.04.016http://www.sciencedirect.com/science/article/pii/S0301421514002328.
[7] Worthmann K, Kellett CM, Braun P, Grne L, Weller SR. Distributed and decentralized control of residential energy systems incorporating battery storage. IEEE Trans Smart Grid 2015;6(4):1914–23. https://doi.org/10.1109/TSG.2015.2392081.
[8] Vieira FM, Moura PS, de Almeida AT. Energy storage system for self-consumption of photovoltaic energy in residential zero energy buildings. Renew Energy 2017;103:308–20. https://doi.org/10.1016/j.renene.2016.11.048http://www.sciencedirect.com/science/article/pii/S0960148116310321.
[9] Kumar S, Chandiwala S, Khare VR, Pant M. Integrating energy efficiency with renewables and energy storage for a smarter and greener residential solution. In: Pillai RK, Ghatikar G, Seethapathy R, Sonavane VL, Khaparde SA, Yemula PK, Chaudhuri S, Venkateswaran A, editors. ISGW 2017: compendium of technical papers. Singapore: Springer Singapore; 2018. p. 231–5.
[10] Lam RK, Tran DH, Yeh HG. Economics of residential energy arbitrage in california using a PV system with directly connected energy storage. 2015 IEEE Green Energy and Systems Conference (IGESC) 2015. p. 67–79. https://doi.org/10.1109/IGESC.2015.7359453.
[11] Kabir M, Mishra Y, Ledwich G, Dong ZY, Wong KP. Coordinated control of grid-connected photovoltaic reactive power and battery energy storage systems to improve the voltage profile of a residential distribution feeder. IEEE Trans Ind Inform 2014;10(2):967–77.
[12] Parisio A, Rikos E, Glielmo L. A model predictive control approach to microgrid operation optimization. IEEE Trans Control Syst Technol 2014;22(5):1813–27. https://doi.org/10.1109/TCST.2013.2295737.
[13] Koohi-Kamali S, Rahim N, Mokhlis H. Smart power management algorithm in microgrid consisting of photovoltaic, diesel, and battery storage plants considering variations in sunlight, temperature, and load. Energy Convers Manage 2014;84:562–82.
[14] Das A, Ni Z. A computationally efficient optimization approach for battery systems in islanded microgrid. IEEE Trans Smart Grid.
[15] Abushnaf J, Rassau A. Impact of energy management system on the sizing of a grid-connected pv/battery system. Electr J 2018;31(2):58–66. https://doi.org/10.1016/j.tej.2018.02.009http://www.sciencedirect.com/science/article/pii/S1040619017302798.
[16] Keck F, Lenzen M, Vassallo A, Li M. The impact of battery energy storage for renewable energy power grids in australia. Energy. doi:https://doi.org/10.1016/j.energy.2019.02.053. < http://www.sciencedirect.com/science/article/pii/S0360544219302427 > .
[17] Wolfs P, Reddy GS. A receding predictive horizon approach to the periodic optimization of community battery energy storage systems. 2012 22nd Australasian Universities Power Engineering Conference (AUPEC). IEEE; 2012. p. 1–6.
[18] Ratnam EL, Weller SR. Receding horizon optimization-based approaches to managing supply voltages and power flows in a distribution grid with battery storage co-located with solar pv. Appl Energy 2018;210:1017–26.
[19] de Groot RJ, Vonk BM, Beckers HJ, Slootweg JG. Development of a charge path optimization controller block for a battery energy storage system. IFAC Proc Vol 2014;47(3):8583–7.
[20] De Groot R, Van Overbeeke F, Schouwenaar S, Slootweg H. Smart storage in the enexis lv distribution grid. 22nd international conference and exhibition on electricity, distribution, CIRED. 2013.
[21] van Dun JJCM, de Groot RJW, Morren J, Slootweg JG. Control of a battery energy storage system connected to a low voltage grid. 2015 IEEE Eindhoven PowerTech 2015. p. 1–6. https://doi.org/10.1109/PTC.2015.7232405.
[22] Le Nguyen H. Newton-raphson method in complex form [power system load flow analysis]. IEEE Trans Power Syst 1997;12(3):1355–9.
[23] Kersting WH. Distribution system modeling and analysis. CRC Press; 2001.
[24] Kirtley J. 6.061 Introduction to power systems class notes chapter 5 introduction to load flow, MIT open courseware; 2018. < https://ocw.mit.edu/courses/electrical-engineering-and-computer-science/6-061-introduction-to-electric-power-systems-spring-2011/readings/MIT6_061S11_ch5.pdf > .
[25] van Westering W, Droste B, Hellendoorn H. Combined medium voltage and low voltage simulation to accurately determine the location of voltage problems in large grids. In: 2019 CIRED; 2019. p. 2.

[26] Military R, Popa I. On the numerical solving of complex linear systems. Int J Pure Appl Math 2012;76:113–22http://ijpam.eu/contents/2012-76-1/11/11.pdf.
[27] Dobbe R, van Westering W, Liu S, Arnold D, Callaway D, Tomlin C. Forecasting-based state estimation for three-phase distribution systems with limited sensing. IEEE Trans Power Syst [under review].
[28] M.E.V. Team. A guide to understanding battery specifications. MIT; 2018. < http://web.mit.edu/evt/summary_battery_specifications.pdf > .
[29] Tan NML, Abe T, Akagi H. A 6-kw, 2-kWh lithium-ion battery energy storage system using a bidirectional isolated dc-dc converter. In: The 2010 international power electronics conference – ECCE ASIA; 2010. p. 46–52. doi:https://doi.org/10.1109/IPEC.2010.5543647.